OBSERVATIONS OF MF-HF PLASMA WAVE EMISSIONS IN THE POLAR IONOSPHERE USING THE ANTARCTIC ROCKETS S-310JA-4 AND S-310JA-6

Hiroshi MIYAOKA, Hiroshi OYA

Geophysical Institute, Tohoku University, Sendai 980

and

Sadao MIYATAKE

University of Electro-Communications, 5-1, Chofugaoka 1-chome, Chofu 182

Abstract: Using Antarctic rockets S-310JA-4 and S-310JA-6 launched respectively on August 18 and August 27 in 1978, plasma waves in the MF and HF frequency range, *i.e.*, from 0.1 MHz to 10 MHz have been observed in the polar ionospheric level up to 230 km. Four categories of the plasma wave emissions are identified in consideration of the correlation with the energetic particles data. The first is the subsidiary emissions that are enhanced in the form of the ESCH (electrostatic electron cyclotron harmonic) waves due to the energetic electron beams in 2 keV range; the emissions are generated in a regime of the nonlinear wave particle interactions because of the effective growth rate of the ESCH waves. The second is the ESLEC mode waves. The electrostatic plasma waves in the frequency range lower than the electron cyclotron frequency are called ESLEC mode waves in this paper; the generation of ESLEC mode wave is caused by the loss-cone type velocity distribution of the particles without any significant relationship to the electron beams in auroras. The third is the wide-band emission that can be attributed to the continuum emission emanating from the upper side of the ionosphere located below the rocket position; there still remains a possibility of the celestial radio waves arriving from the outside of the earth. The fourth is the leaked auroral kilometric radiation (AKR), propagating down towards the ionosphere in the form of the whistler mode waves. The waves have no one-to-one correspondency to the *in situ* observations of the precipitating particles, but the source is located in the region of the auroral particle accelerations where the AKR is generated.

1. Introduction

The region of the polar ionosphere is an important field for the study of the plasma wave phenomena relating to the development of auroras. It is well established that the magnetospheric substorm induces the auroral breakup in the lower part of the polar ionosphere by precipitating the energetic particles. In addition to the luminating activity through the photochemical processes due to the encounter

with the neutral upper atmosphere, *i.e.*, the production of the auroras, there are expected vital activities of the interaction between the precipitating particles and the ionospheric plasma. The plasma wave phenomena in the polar ionosphere, however, are not restricted to the *in situ* effect due to the precipitating auroral particles, but can cover a relatively wide range of the space where the auroral particles are concerned. The study of the plasma wave observations in these areas, thus, has complicated feature and indicates a wide variety of characteristics. The investigation of the waves and particles phenomena in the polar ionosphere, however, provides us with the important key to discern the microscopic aspect and the macroscopic range of the plasma phenomena in the auroral region associated with the evolution of the magnetospheric substorms that are intimately connected with the auroral activities.

The previous studies on the plasma waves were rather confined to the field of the whistler mode waves in VLF range (lower than 30 kHz). Only a few observations were carried out in MF or HF range in the past (KELLOGG and MONSON, 1978, 1979). They indicated the possibility of the beam-plasma instabilities with *in situ* nature.

In the period of the International Magnetospheric Study (IMS), 1976–1980, a series of rocket experiments for the purpose of investigating the wave-particle interaction in the auroras have been performed at Syowa Station in Antarctica by the National Institute of Polar Research. Instruments to measure a plasma wave spectrum in the high frequency range (named PWH) were installed and made successful observations by means of S-310JA-1, S-210JA-20 and S-210JA-21 as the first rocket experiment of this series in 1976 by the 17th Japanese Antarctic Research Expedition (JARE-17), followed by the launching of S-310JA-2 rocket in 1977 by JARE-18 as the second experiment. These experiments have shown the existence of electrostatic plasma waves near the upper hybrid frequency and a half of the electron cyclotron frequency in the lower ionosphere at a low altitude down to 100 km (OYA *et al.*, 1979, 1980).

The succeeding third experiments, using the Antarctic rockets S-310JA-4 and S-310JA-6 were carried out on August 18 and 27 in 1978, respectively, by JARE-19. In addition to PWH, these rockets were equipped with an electron density probe and an electron temperature probe (named NEI, TEL), an energetic electron counter (named ESM) and a VLF wide-band receiver (named EMF, PWL), to clarify the interaction between the waves (from VLF to HF range) and the energetic particles phenomena in the auroras.

The purpose of the present paper is to describe the characteristics of the plasma waves observed by these two rocket experiments that led us to important discoveries of the MF and HF phenomena in the polar ionosphere. From the investigation of the frequency relations between the plasma waves and the plasma characteristic frequencies, we determine the mode of these plasma waves. The generation mechanisms of these emissions are studied by comparing the flux data of energetic electrons relating to the auroras observed on the same rockets simultaneously.

2. Instrumentation of the PWH Experiment

The block diagrams of PWH (plasma wave detector in HF range) installed on the
S-310JA-4 and S-310JA-6 rockets are shown in Figs. 1a and 1b. PWH system in-
struments on the rockets consist of the following three parts; a 1.2 m whip antenna, a
wide band and medium gain pre-amplifier, and a swept-frequency type (super hetero-
dyne) receiver, although each part has modifications in detailed portion between the
two rocket experiments.   One of large modifications of the PWH system on S-310JA-
4 is that an impedance probe for the measurement of the number density of electrons
(NEI) is attached making one organized system; PWH and NEI equipments are oper-
ated making time share with intervals of 8 s for PWH and 2 s for NEI.   The electric
field component of MF-HF radio waves picked up by the 1.2 m antenna is fed into
the swept-frequency receiver through the pre-amplifier.   The output signal from
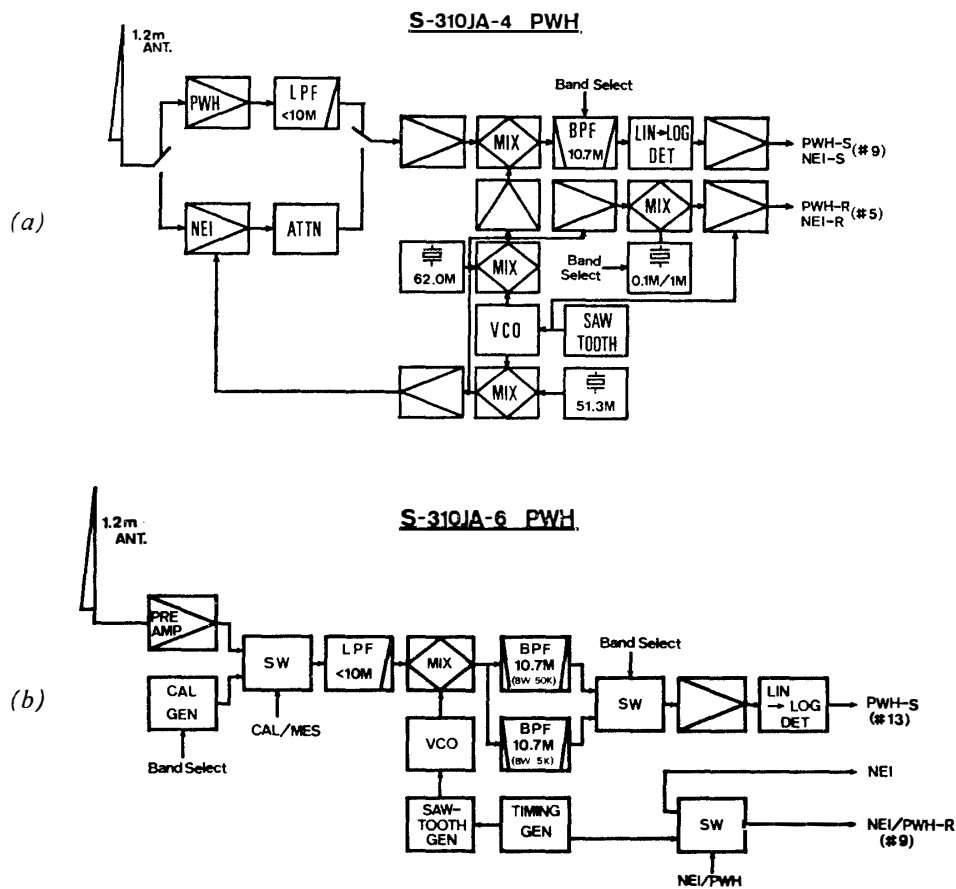the pre-amplifier is further fed into a spectrum analyzer where the spectrum of the

Fig. 1.   Block diagram of PWH instruments on board S-310JA-4 (a) and S-310JA-6 (b) rockets.

Table 1.   Parameters of PWH on board S-310JA-4 and S-310JA-6.

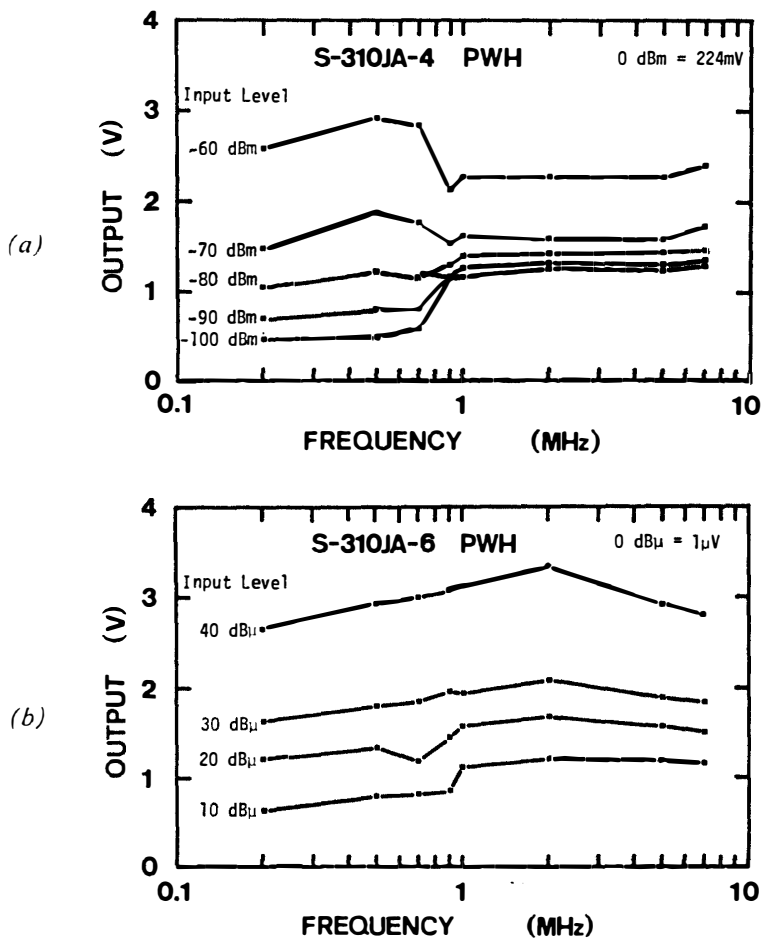|		S-310JA-4	S-310JA-6
Frequency range	(Low)	0.1–1 MHz	0.1–1 MHz
	(High)	1–10 MHz	1–10 MHz
Sweet time	(Low)	1 s	0.25 s
	(High)	1 s	0.25 s
Band width	(Low)	5 kHz	5 kHz
	(High)	50 kHz	50 kHz
Sensitivity		5 μV	1.8 μV
Dynamic range		60 dB	50 dB
Antenna		1.2 m whip	1.2 m whip
TM channel	(PWH-S)	IRIG #9	IRIG #13
	(PWH-R)	#5	#9

(a)

(b)

Fig. 2.   Overall frequency characteristics of PWH systems on board S-310JA-4 (a) and S-310JA-6 (b) rockets.

signal is detected in a frequency range from 100 kHz to 10 MHz in every 2 s for the case of S-310JA-4, and in every 0.5 s for the case of S-310JA-6.

The swept-frequency analyzer consists of the super heterodyne receiver where the local frequency is swept from 10.8 MHz to 20.7 MHz to make the intermediate frequency (IF) at 10.7 MHz. The bandwidth of the IF stage is 5 kHz in the lower frequency range (0.1–1 MHz), and 50 kHz in the higher frequency range (1–10 MHz) for both the rocket experiments. The other characteristic parameters of PWH systems are summarized in Table 1.

The calibration of the overall frequency characteristics of the PWH systems was carried out in the pre-flight test; the results are shown in Figs. 2a and 2b for S-310JA-4 and S-310JA-6, respectively.

3. Results of the S-310JA-4 Experiment

The S-310JA-4 rocket was launched at 033243 LT (45°E) on August 18, 1978 in the anti-parallel direction of the geomagnetic field vector, and reached the maximum altitude of 195 km at 220 s after the launch. The flight was made just after the onset of the substorm as has been given in Fig. 3a. The substorm activity was relativity weak with $\Delta H = -120\gamma$. The cosmic noise absorption (CNA) at 30 MHz was -1 dB; VLF hiss emissions at 0.75, 2 and 8 kHz were clearly observed at Syowa Station.

The observation of auroral intensity at a wavelength 5577 Å by a scanning photometer in the geomagnetic meridian plane (HIRASAWA and NAGATA, 1972) is shown in Fig. 3b, in which the rocket trajectory is projected, along the geomagnetic field line, to the luminating level of the aurora. The rocket trajectory was shifted from the center portion of the auroral breakup region.

Typical PWH data obtained by the S-310JA-4 experiment are shown in Fig. 4. In these data, PWH-R and PWH-S are a channel for the frequency calibration and a channel to send the level of the plasma wave intensity, respectively; the PWH-S signal is expressed in a form of the spectrum corresponding to the frequency given in PWH-R, simultaneously. The PWH-S data are, therefore, an A-scan type dynamic spectrum where the frequency axis is expanded *versus* the time. To obtain a two-dimensional format of the dynamic spectra, we have made a data treatment so as to fix the frequency axis in a given resolution time, *i.e.*, 2 s for the S-310JA-4 experiment.

In Fig. 5, an overall view of a data processing system to make dynamic spectra is indicated. The data in the PWH-S channel indicate a remarkable offset level due to the set noise of the receiver. We must, therefore, subtract this offset level from the PWH-S data to make a dynamic spectrum of the observed plasma waves. The spectrum data processed through the subtraction circuit are then fed into the Z-axis (intensity modulation axis) of the CRT display tube. The X-axis of the CRT is swept by a sawtooth signal, and the origin is triggered by the zero-beat signal of the law data. By moving a film, the time dependent variation of the spectrum intensity is
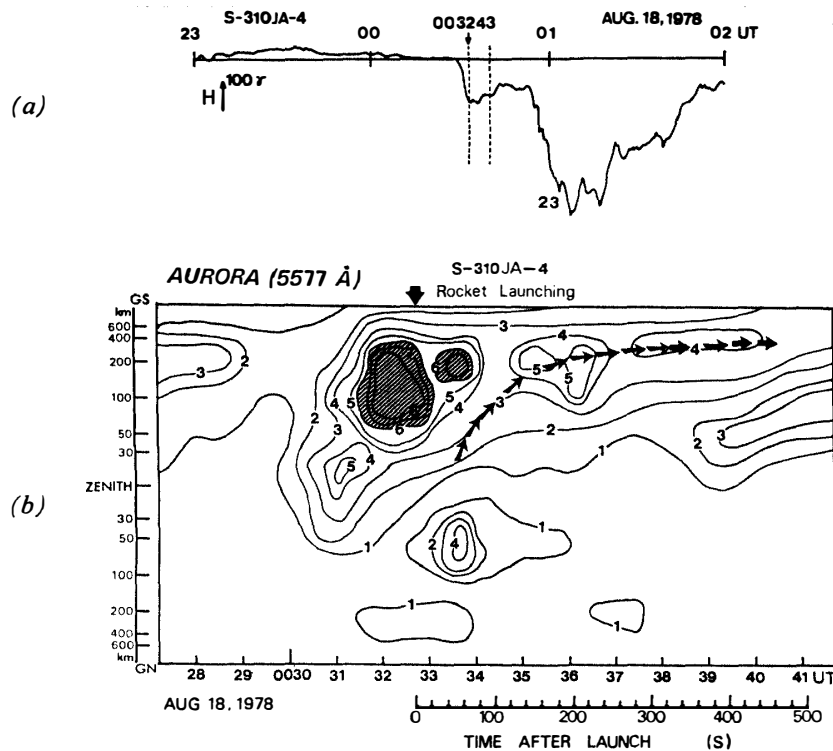
Fig. 3. (a) Geomagnetic field variations of an H-component observed during the S-310JA-4 rocket experiment at Syowa Station.

(b) Auroral intensity at a wavelength 5577 Å observed by the meridian scanning photometer during the S-310JA-4 rocket experiment at Syowa Station (after T. HIRASAWA). The rocket trajectory is projected to the luminating level of auroras along the geomagnetic field line. The rocket was launched just after the onset of a substorm, and took the path into the weak auroral region.

recorded. The dynamic spectrum made by these processes is shown in Fig. 6a, with the energetic particles data (Fig. 6b) and the VLF dynamic spectrum (Fig. 6c) obtained on the same rocket simultaneously.

In Fig. 6a, narrow band lines at 0.25, 2.8, 5.8 and 8.1 MHz are caused by interferences in the receiver. Except for these interference lines, a diffuse, band-limited emission with a center frequency near 200 kHz is observed almost constantly over a 100 km level. The narrow band waves, observed near 7 and 9 MHz during the up-leg, are considered to be broadcast waves in the HF band that penetrated through the ionosphere transmitted from ground stations.

In the S-310JA-4 experiment, the activity of the in situ plasma wave phenomena was rather weak compared with the previous observations (OYA et al., 1979, 1980). The diffuse emission near 200 kHz was the only natural emission. The detailed description of this emission will be given in Section 9. The possible causes for which
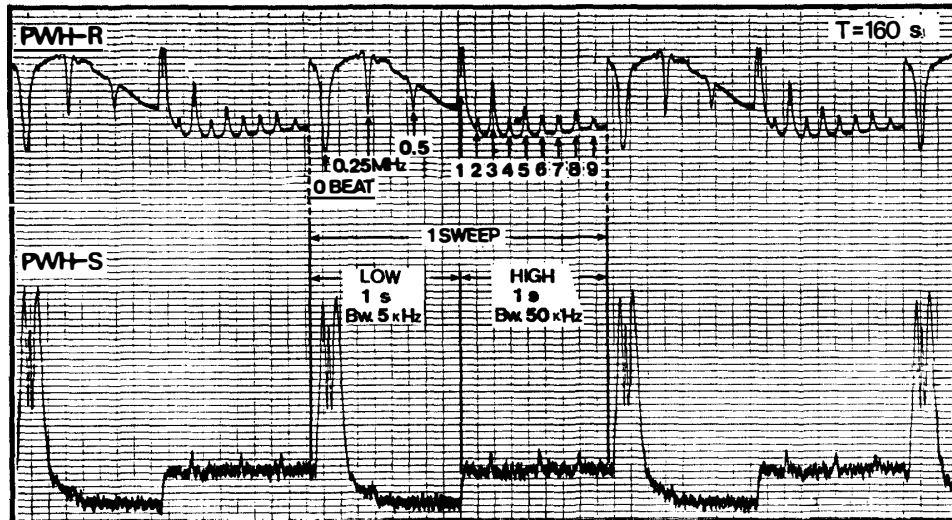
Fig. 4. Typical PWH data obtained by the S-310JA-4 experiment. PWH-R and PWH-S are the channel for the frequency calibration and the channel to send the level of the plasma wave intensity, respectively; measured plasma wave data in PWH-S sent in a form of spectrum coincide with the swept frequency ranging from 100 kHz to 10 MHz as given in PWH-R channel in every 2 s.
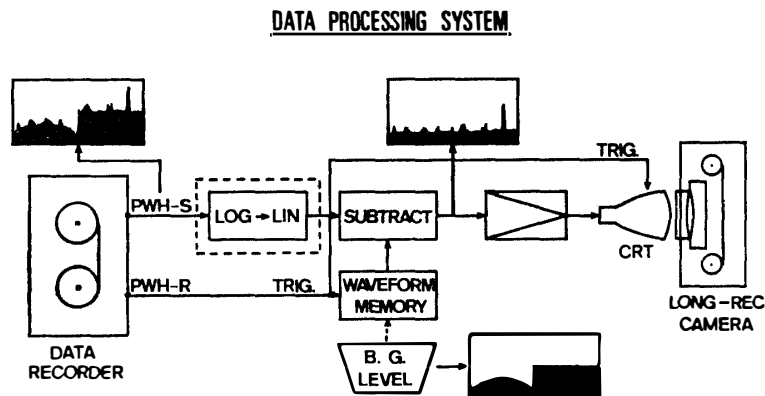
DATA PROCESSING SYSTEM

Fig. 5. Data processing system on the ground used to make the dynamic spectra of the plasma waves.

we could not observe the *in situ* plasma waves are as follows: i) The rocket flight was made during the relatively weak geomagnetic and auroral activity as indicated in Fig. 3, ii) the rocket path was shifted from the main portion of the auroral break-up, and iii) the receiver gain of the PWH system had been dropped by 6 dB compared with the situation in the calibration period.

The dynamic spectrum observed by PWH is compared with the flux data of
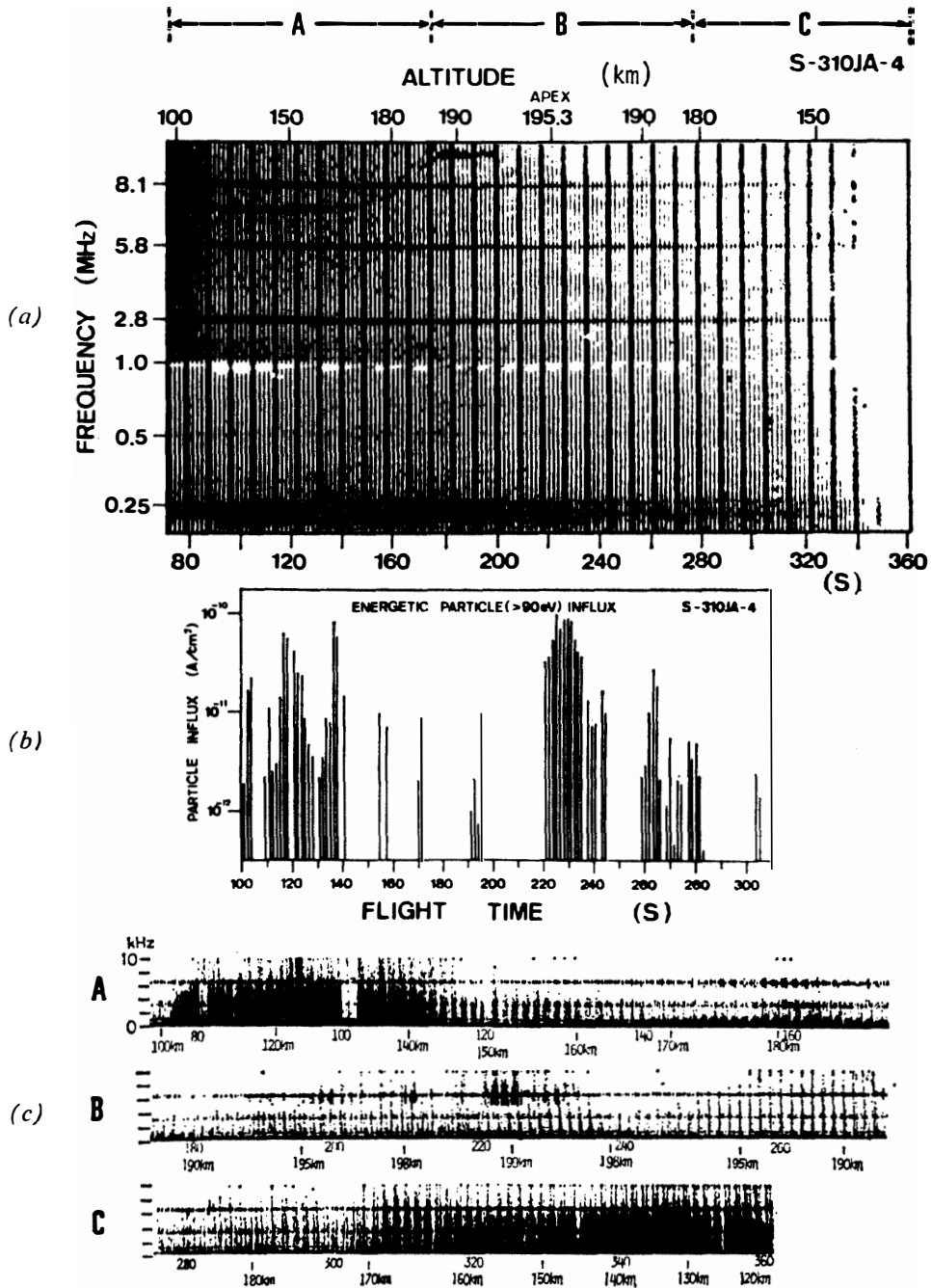
Fig. 6.   (a)   Dynamic spectrum of the plasma waves in the frequency range from 100 kHz to
10 MHz observed by S-310JA-4.
(b)   Flux of the energetic particles in the energy range over 90 eV observed by the
Farady-Cup analyzer on board S-310JA-4 (after M. EJIRI).
(c)   Dynamic spectrum of the VLF plasma waves observed by the same rocket simul-
taneously (after H. YAMAGISHI et al.).

energetic particles observed by a Farady-Cup analyzer, and the VLF dynamic spectrum obtained by a wide-band VLF receiver covering up to 10 kHz, as shown in Figs. 6b and 6c.   As has been indicated in Fig. 6b, the energetic particle influx which has the energy over 90 eV was enhanced in the following periods, 100–140 s, 220–240 s and 260–280 s.   Although there is no clear correlation between the MF diffuse emission (see Fig. 6a) and the flux enhancements of energetic particles, the emitted VLF plasma waves (see Fig. 6c) are clearly correlated with the precipitating particles around 220 s after the launch.

4. Results of the S-310JA-6 Experiment

The S-310JA-6 rocket was launched at 005600 LT (45°E) on August 28, 1978 in the direction parallel to the geomagnetic field vector, and reached the maximum altitude of 237 km at 240 s after the launch.   The flight was made during the transition period from the onset to the expansion phase of the substorm with a medium level of the geomagnetic variation ($\Delta H = -220\gamma$, see Fig. 7a).   The cosmic noise absorption (CNA) at 30 MHz was -1.5 dB and VLF hiss emissions at 8 kHz were observed on the ground (Syowa Station).   Results of these ground observations are summarized in Table 2 including the case of the S-310JA-4 flight.

In Fig. 7b, the observed auroral activity at 5577 Å (Hirasawa and Nagata, 1972) is shown with the flight path of the S-310JA-6 rocket; the path is projected, again, on the luminating level of the aurora traced along the geomagnetic field line. The flight was made around the edge region of the maximum activity of the auroral breakup.

The dynamic spectrum of the plasma waves in a frequency range from MF to HF range observed by the S-310JA-6 rocket experiment is shown in Fig. 8a.   The data are contaminated in this experiment by the interference of the NEI (impedance probe) equipment.   The leakage of the swept-frequency RF signal from the impedance probe entered the PWH receiver at a frequency which coincides with the receiving frequency of the PWH system; the results make the white points forming the slant patterns (see Fig. 8a).   In Fig. 8b, the data are modified by removing the white points of the interference RF signals.   A schematic illustration of the dynamic spectrum is given in Fig. 8c; in this diagram, the electron plasma frequency F_P and the electron cyclotron frequency F_H are also plotted to compare the frequency relations with the frequency of the observed plasma wave emissions.

In Figs. 8a, 8b and 8c, narrow band emissions near 6, 7 and 9 MHz are broadcast radio waves from ground stations.   It is interesting that these broadcast radio waves were observed at the topside of the ionosphere with a peak plasma frequency of about 7 MHz, as well as in the lower ionosphere.   This result can be interpreted as follows: The electron density at the altitude of about 100 km was locally enhanced due to the precipitating particles connected with the auroral breakup around the
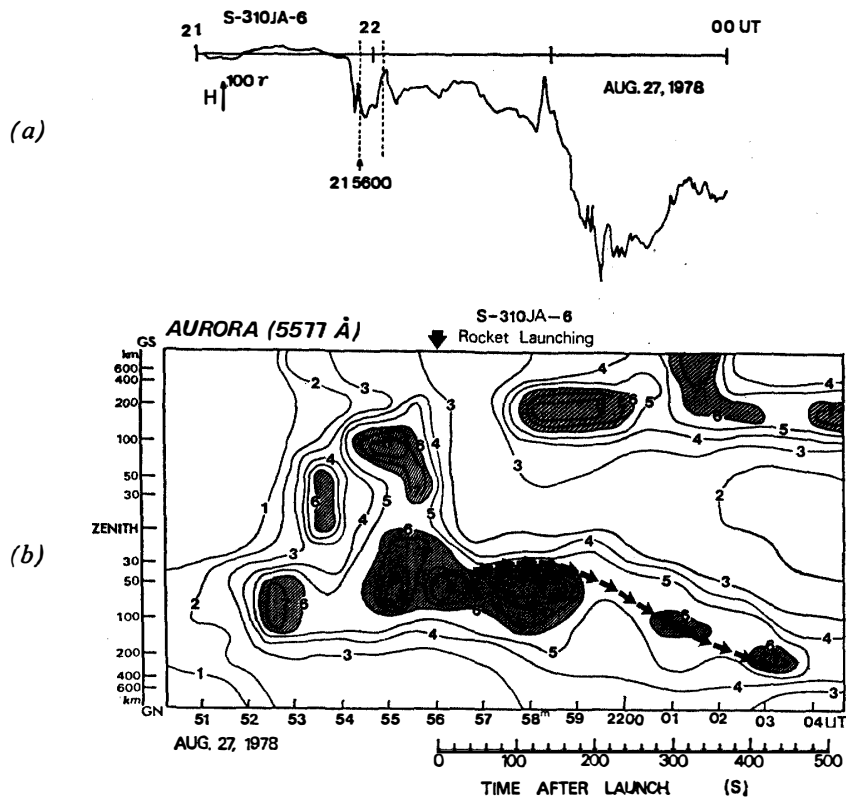
Fig. 7. (a) Geomagnetic field variation of an H-component observed during the S-310JA-6 rocket experiment at Syowa Station.

(b) Auroral intensity at a wavelength 5577 Å observed by the meridian scanning photometer during the S-310JA-6 rocket experiment at Syowa Station (after T. HIRA-SAWA). The rocket trajectory is projected in the same format as Fig. 3b. The rocket was launched during the transition period from the onset to the expansion phase of a substorm, and took the path around the edge region of the maximum activity of the auroral breakup.

Table 2. Summary of ground observations at the time of rocket launching.

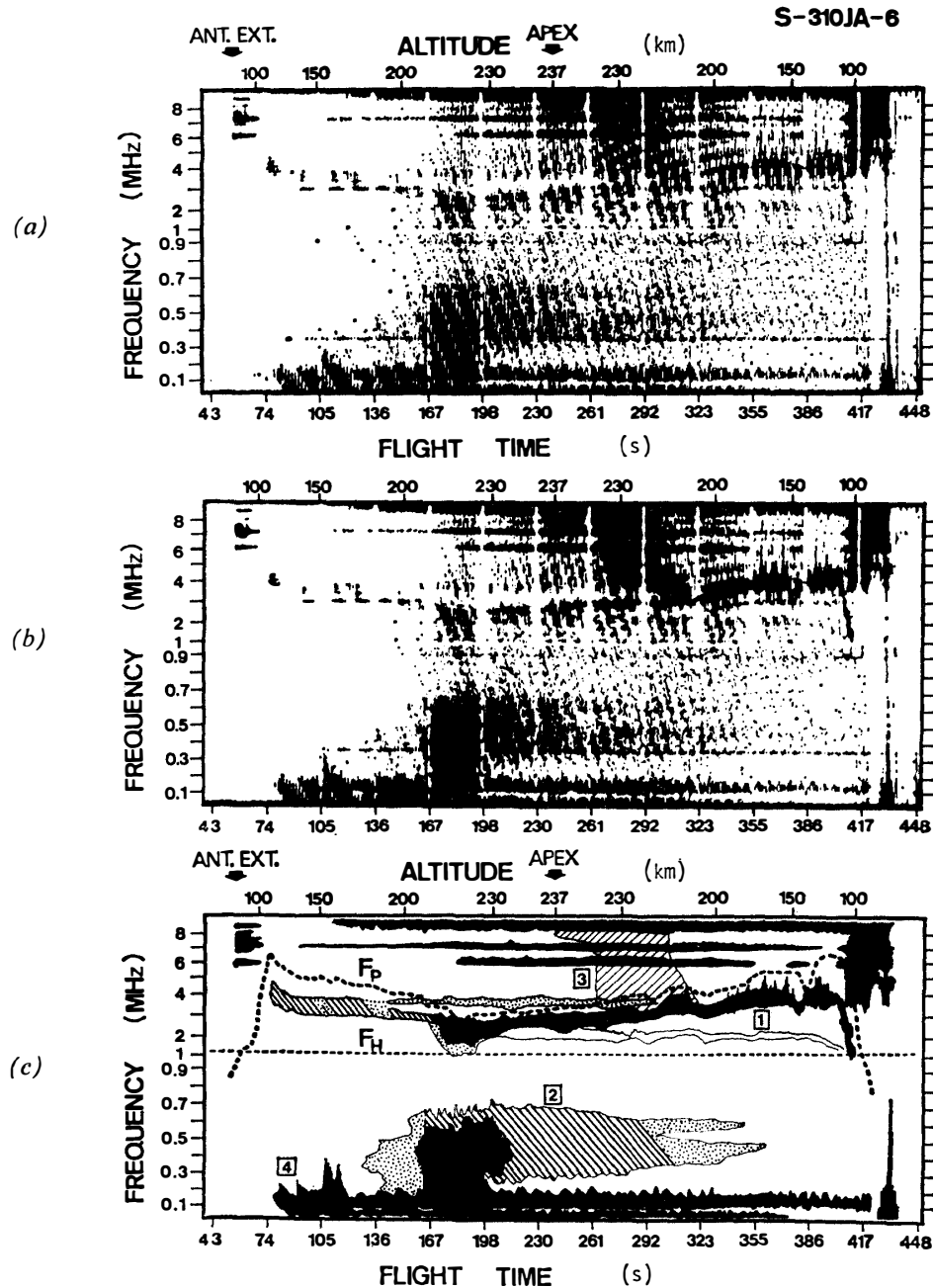| Items	S-310JA-4	S-310JA-6
Date/Time	August 18, 1978, 003243 UT	August 27, 1978, 215600 UT
Direction of launching	Geomagnetic south	Geomagnetic north
ΔH	-120γ	-220γ
Pulsation	Pi2 (moderate)	Pi2 (active)
CNA (30 MHz)	-1 dB	-1.5 dB
VLF	0.75, 2, 8 kHz hiss	8 kHz hiss
Aurora	Weak	Intense
Substorm phase	Onset	Expansion
Kp (ΣKp)	$3+$ $(26-)$	$4+$ $(33-)$

Fig. 8.   (a)   Dynamic spectrum of the plasma waves in the frequency range from 100 kHz to 10 MHz observed by S-310JA-6.
(b)   Same as (a) after the correction on the interference from NEI instrument.
(c)   Schematic illustration of the dynamic spectrum shown in (a) and (b).   The electron plasma frequency F_P observed by NEI and the electron cyclotron frequency F_H calculated from IGRF (1975) model are also plotted.

rocket flight path. The broadcast radio waves observed at the topside of the ionosphere, therefore, must have penetrated into the ionosphere through the ionospheric region with the lower electron density located apart from the rocket path, where no severe particle precipitation took place. That is, these phenomena can be attributed to the horizontal inhomogeneity of the maximum electron density in the ionosphere.

Except for these broadcast radio waves, we can find four kinds of natural plasma wave emissions in the dynamic spectrum shown in Fig. 8. These emissions are classified into four types as follows.

1) *Type 1 emission*: A band-limited emission which was observed just below the electron plasma frequency F_P (labeled 1 in Fig. 8c). This emission was observed almost through the whole period above the 100 km level, especially clearly after about 170 s. The intensification of the Type 1 emission in the period of 320–400 s was associated with the enhancement of precipitating electrons, as will be explained later. The Z-mode cutoff frequency $F_{L=0}$ was lower than F_P by about 0.5 F_H in this case. Because most of the Type 1 emission was observed at the frequency below $F_{L=0}$, it can be concluded that this Type 1 emission belongs to the electrostatic electron cyclotron harmonic (ESCH) mode.

2) *Type 2 emission*: A diffuse, broad-band emission which was observed around a half electron cyclotron frequency 0.5 F_H (labeled 2 in Fig. 8c). This emission was intensified suddenly at about 160 s, and grew weaker monotonously with time making the bandwidth narrower. Because the frequency domain of the Type 2 emission is located below F_H, this emission is considered to be possibly the whistler mode or the electrostatic mode with the frequency lower than the electron cyclotron frequency. The same emission as this Type 2 emission has been also observed in the previous rocket experiment (OYA *et al.*, 1980).

3) *Type 3 emission*: A broad-band emission which appeared in the period from 260 to 320 s in a frequency range above 3 MHz (labeled 3 in Fig. 8c). The lower cutoff of this emission seems to coincide with the local electron plasma frequency or the Z-mode cutoff frequency; it is concluded that the emission belongs to the electromagnetic mode in a plasma. There are two possible candidates for this emission: The first is an L-O mode electromagnetic wave which has been converted from an electrostatic plasma wave excited locally by the precipitating electrons in the ionosphere nearly at the upper hybrid frequency. The second is a Type III solar radio burst in the HF band which is observed frequently accompanied by a solar flare above the ionosphere. We will make a detailed discussion on this emission mechanism in the next section.

4) *Type 4 emission*: A narrow-band emission which was observed constantly in a frequency range from 100 kHz to 200 kHz during almost the whole period over the 100 km level of the rocket flight (labeled 4 in Fig. 8c). The bandwidth and the intensity of this emission were rather large, contrary to the Type 1 emission, in the

up-leg.   The mode of the Type 4 emission is evidently the whistler mode considering the emission frequency.

The four kinds of emissions observed in this experiment are considered to be the essential plasma wave phenomena in the polar ionosphere, especially in active auroras. The investigation of the generation mechanism of these emissions, therefore, should give us valuable information on the wave-particle interactions in the auroral region.

5. Wave and Particle Conditions during the Experiments

The dispersion curves of the plasma waves covering a whole domain of wavelengths from electromagnetic waves to electrostatic waves have been calculated based on the same background as the previous work (OYA, 1971), using the observed plasma parameters by NEI (for the electron number density) and TEL (for the electron temperature).   The results of the observations by NEI and TEL are both indicated in summary diagrams of plasma parameters shown in Figs. 9a and 9b for the case of S-310JA-4 and S-310JA-6 rocket experiments, respectively.   In Fig. 10, the calculated dispersion curves are given for the plasma parameter corresponding to the apex of the S-310JA-6 rocket flight path; i.e., $F_P/F_H = 4$ and $T_e = 2000$ K.
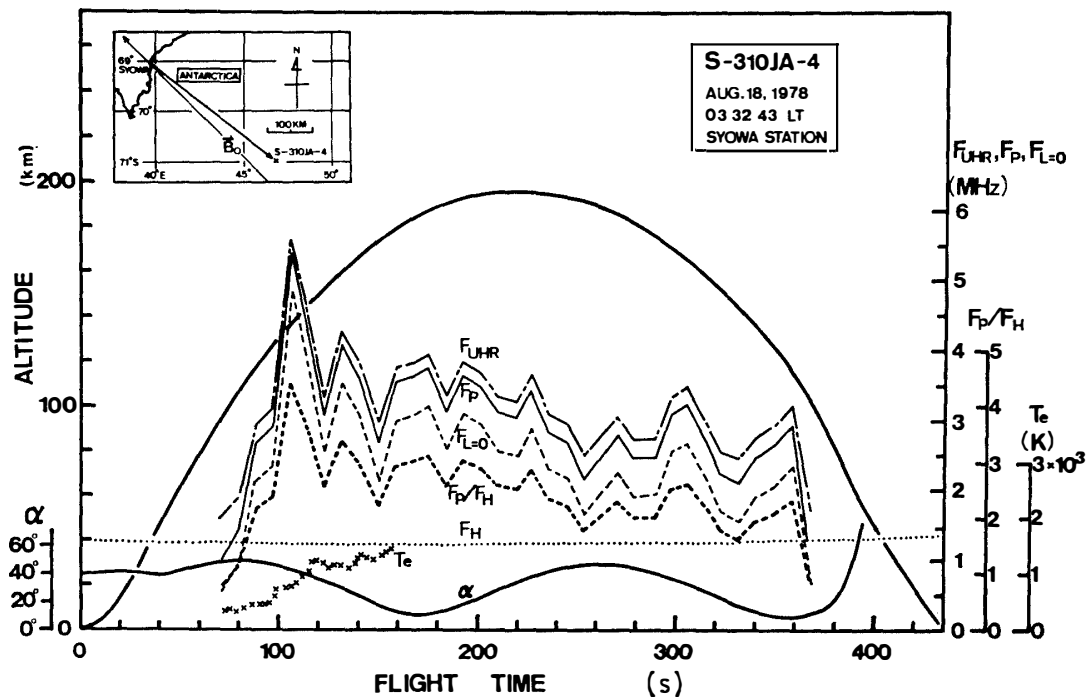

Fig. 9a. Summary diagram of plasma parameters in the S-310JA-4 experiment. The characteristic frequencies, such as F_{UHR}, F_P, $F_{L=0}$, F_H and F_P/F_H, and the temperature T_e are plotted versus rocket flight time.   The rocket trajectory and the angle α between the spin axis and the geomagnetic field are also indicated.
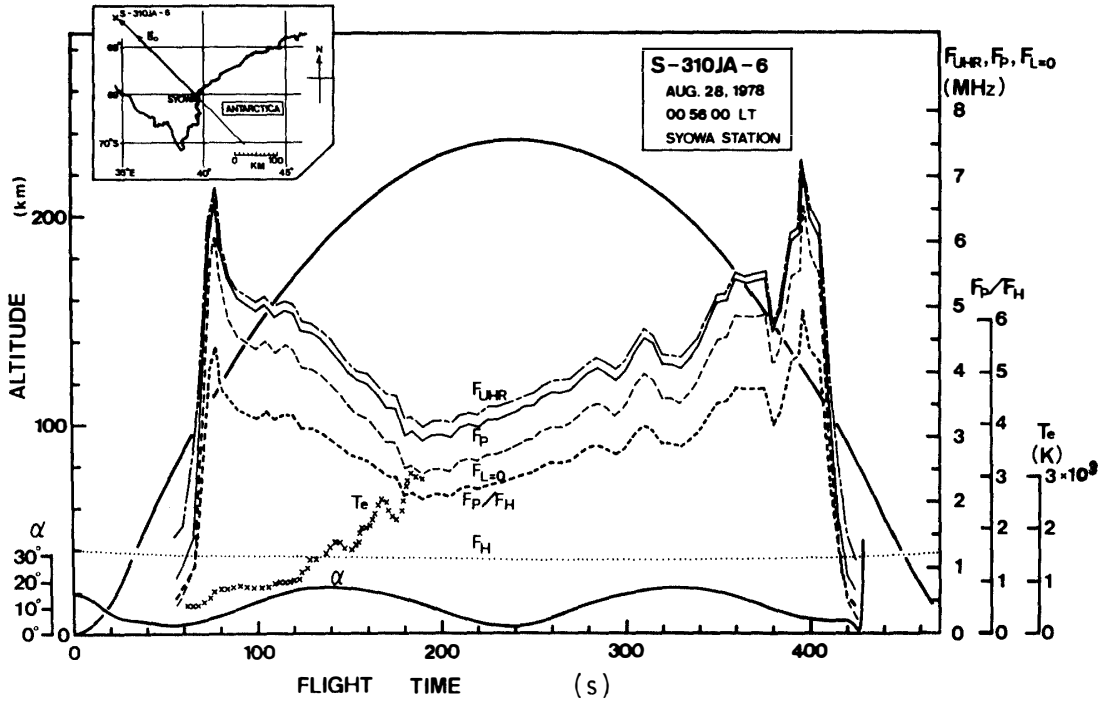
Fig. 9b.   Same as (a) for the S-310JA-6 experiment.

The frequency coverage of the PWH system from 100 kHz to 10 MHz corresponds to the range approximately from 0.1 F_H to 9 F_H for the electron cyclotron frequency $F_H = 1.2$ MHz, which was almost constant during the observations (see Fig. 10). This frequency coverage includes most branches of the plasma waves from the electromagnetic to the electrostatic waves in a magnetoactive plasma; *i.e.*, the whistler mode waves, the electrostatic electron cyclotron harmonic (ESCH) waves, the UHR waves and the electromagnetic waves. The four characteristic emissions observed in these experiments (*i.e.*, from Type 1 to Type 4) can be categorized into either of them.

The condition of the Landau type wave-particle resonant interaction is expressed as,

$$\omega - \mathbf{k} \cdot V_b = 0 \tag{1}$$

where ω, $\mathbf{k}$ and V_b are the angular frequency of the waves, the wave number vector and the field-aligned component of the electron beam velocity, respectively. In Fig. 10, this condition is illustrated by broken lines. Four cases of the parameter $(V_b/V_{th})\cos\theta = 1$, 10, 10^2 and 10^3 are indicated in the diagram, where θ is the angle between the wave number vector and the magnetic field. At the cross-points, the plasma wave with corresponding $(\omega, \mathbf{k})$ values can be excited as a process of the inverse Landau damping, when the electron beam has a sufficient flux. In Fig. 10, the beam
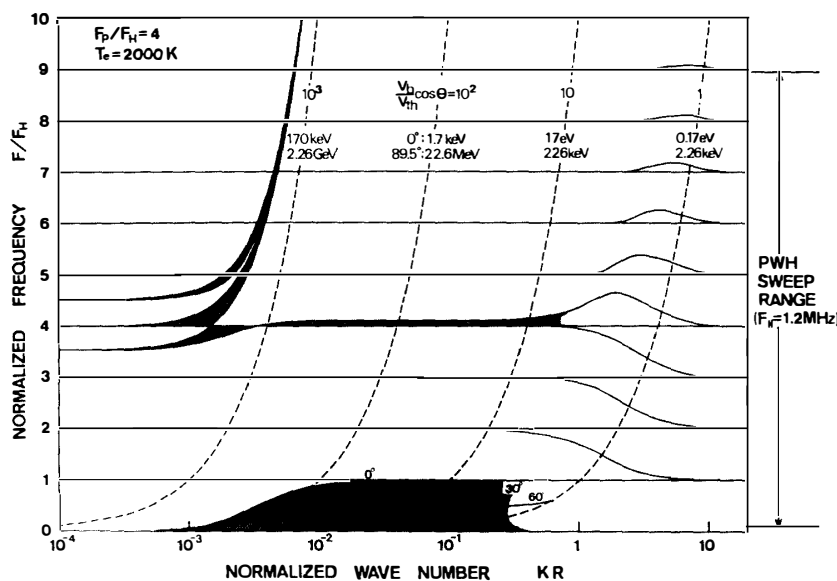
Fig. 10. ω k digram of the plasma waves in a warm magnetoactive plasma. The plasma parameter F_P/F_H and the electron temperature T_e used for this calculation are $F_P/F_H = 4$ and $T_e = 2000$ K, for the typical values in the ionosphere near the apex of the trajectory in the S-310JA-6 experiments. The Landau type resonance condition is indicated by broken lines for $(V_b/V_{th})\cos\theta$ values as a parameter. The auroral electrons with the energy of several keV are expected to excite the plasma waves in the electrostatic regime with a large k value.

energy corresponding to $(V_b/V_{th})\cos\theta = 1$ is given for two extreme directions as; 0.17 eV for $\theta = 0°$ and 2.26 keV for $\theta = 89.5°$. For the case of $(V_b/V_{th})\cos\theta = 10^2$, the beam energy is 1.7 keV for $\theta = 0°$ and 22.6 MeV for $\theta = 89.5°$. Thus, the auroral electron beams which have the typical energy of several keV are expected to excite the ESCH waves (including Bernstein waves) in the k-direction which is almost perpendicular to the magnetic field. When the wave normal is directed with an increasing component parallel to the magnetic field, the beams excite the UHR waves, which exist in the frequency range, $F_P < F < F_{UHR}$, and the electrostatic plasma waves with the frequency lower than the electron cyclotron frequency; we call this, hereafter, ESLEC mode waves.

The precipitating electrons that provide V_b are measured simultaneously by ESM (energy spectrum in medium energy range) equipment. The flux data of energetic electrons obtained by ESM in the S-310JA-6 experiment are shown in Fig. 11, for four energy ranges from about 1 keV to 5 keV with two pitch angle directions, i.e., nearly parallel ($3.5° < \alpha < 17.5°$) and perpendicular ($\alpha = 90°$) to the geomagnetic field line. The nature of the pitch angle anisotropy is classified into two categories in Fig. 11. The first is 'trapped' nature as indicated by hatched straight lines, where the electron flux with a pitch angle of 90° is predominant. The second is, on the

ALTITUDE (km)

Fig. 11. Flux of the energetic electrons observed by ESM on board S-310JA-6 in the four energy range from 1 keV to 5 keV. Flux of each energy range is measured in two pitch angle directions, i.e., nearly parallel $(3.5° < \alpha < 17.5°)$ and perpendicular $(\alpha = 90°)$ to the geomagnetic field line. The observation period of the trapped type pitch angle anisotropy, enhanced in the perpendicular direction, is indicated by hatched straight lines. The period of the field-aligned type anisotropy is indicated by shadowed area.
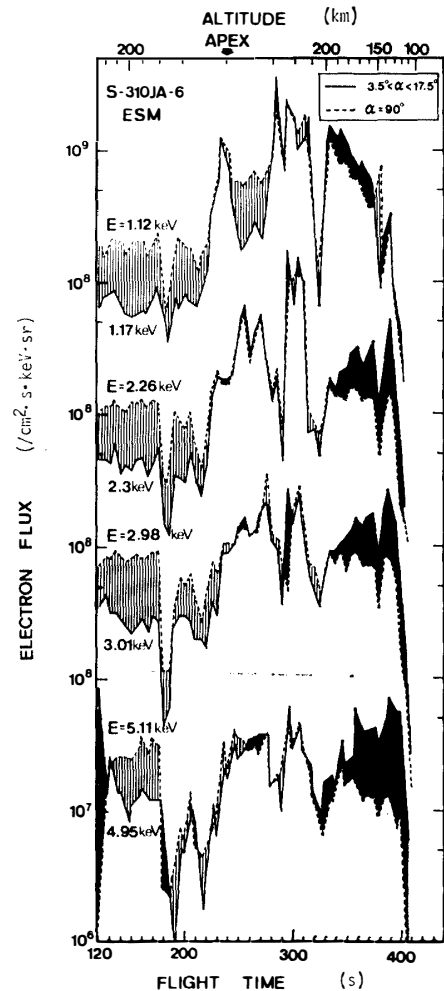
contrary, 'precipitating' nature indicated by a shadowed area, where the electron flux with a pitch angle in $3.5° < \alpha < 17.5°$ is predominant.

From Fig. 11, characteristics of the energetic electron flux, which was responsible for the excitation of plasma waves observed by the *in situ* measurement, are summarized as follows.

1) The flux of energetic electrons increased remarkably in the descent path for both trapped and precipitating components, especially in periods from 230 to 280 s, from 290 to 320 s, and from 340 to 390 s. Among these three periods, the flux of the electrons had a maximum value at the interval from 290 to 320 s for the electron energy range from 1 keV to 2 keV.

2) The observed flux data of electrons can be classified clearly into the following three intervals from the nature of pitch angle anisotropy; *i.e.*,

i) 120–240 s: A trapped-type distribution was prevailing over this period. The electron flux in the lower energy range was limited compared with other periods, but in the higher energy range it was almost the same level as other periods.

ii) 240–320 s: A nearly isotropic distribution was prevailing over this period. The electron flux in this period had a maximum value during the whole observation period in all energy channels.

iii) 320–400 s: A precipitating-type distribution, which is enhanced in the field-aligned direction, was prevailing over this period.   Sudden enhancements of the electron flux were observed a few times in all energy channels.

The above-mentioned information about the pitch angle anisotropy, as well as the
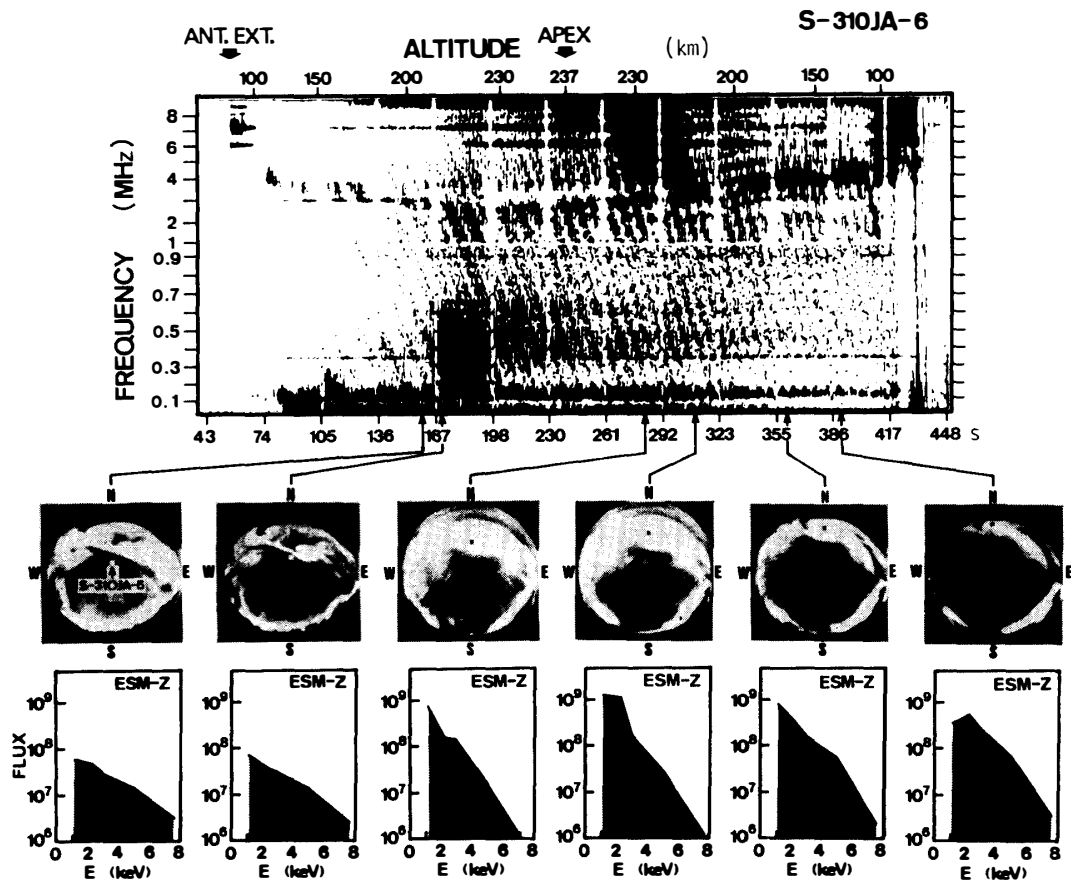

Fig. 12.   Comparison of the dynamic spectrum of the plasma wave emissions with the all-sky photographs of the aurora taken at Syowa Station and with the spectra of the energetic electrons of the field-aligned component $(3.5° < \alpha < 17.5°)$ measured by ESM in the S-310JA-6 experiment.   In the all-sky photographs, the rocket position is projected to the luminating level of auroras along the magnetic field lines.   The spectra of the energetic electrons have a plateau region or a positive-slope region corresponding to the intense Type 1 and Type 3 emissions (see text).

flux value of the energetic electrons, are very significant for the investigation of the generation mechanisms of the observed emissions.

The spectra of energetic electrons of the precipitating component ($3.5° < \alpha <$ $17.5°$), that are responsible for the typical plasma wave emissions, are shown in Fig. 12 together with the all-sky photographs of auroras obtained simultaneously at Syowa Station. In each moment of the all-sky photograph, the position of the S-310JA-6 rocket is indicated by a white or a black spot. The first two electron energy spectra in Fig. 12 were observed when the rocket was located out of an auroral arc, and the others were observed inside the bright aurora. It is clear from Fig. 12 that spectra of the field-aligned component of the energetic electrons have been enhanced remarkably in the low energy range inside the bright aurora. In these cases, the energy spectra have evidently a plateau region ($\partial F(E)/\partial E \simeq 0$) or a positive slope region ($\partial F(E)/\partial E > 0$), where E is the electron energy and $F(E)$ is the eletron energy spectrum. These observations indicate the existence of the field-aligned electron beams with a center energy of about 2 keV. These beams are fairly subjected to the diffusion process that might have resulted from the wave-particle interaction in the auroral plasma. Corresponding to these electron beams, enhancements of the Type 1 and Type 3 emissions are also observed as shown in Fig. 12.

6. Subsidiary Emissions

The Type 1 emission observed by S-310JA-6 has been generated in the following aurora and particle conditions.

1)   Most of Type 1 emissions were observed in the bright auroral arcs.

2)   The enhancements of Type 1 emissions observed in the down-leg after 230 s are associated with the increment of the electron flux with the isotropic or the field-aligned pitch angle distribution (see Figs. 8 and 11).

3)   Type 1 emissions after 320 s indicate, in particular, the close correlation with the field-aligned electron beams whose center energy is approximately 2 keV (see Figs. 11 and 12).

As has been described in Section 4, the mode of the Type 1 emission is identified to be the ESCH mode waves. Since the electron beam with the energy range around 2 keV is responsible for the emission, we should consider the case of the wave propagation nearly perpendicular ($89.5°$) to the magnetic field (see Fig. 10). In Fig. 10, the dispersion curves of the ESCH waves are given only for the case of $\theta = 90°$, but the case is approximately applicable to the case of $\theta = 89.5°$.

The Type 1 emissions are observed in a frequency range lower than F_P with the separation frequency of F_H to $2F_H$ as given in Fig. 8c. These emissions observed by S-310JA-6 are, therefore, basically the same as the Bernstein mode waves in the frequency range either between $3F_H$ and $4F_H$, or between $2F_H$ and $3F_H$.

When we assume the Type 1 emissions to be the ESCH waves, there arises a ques-

tion why the Type 1 emissions are not associated with the other harmonic branches of the ESCH waves, and why there is a clear frequency gap with F_H or $2F_H$ between F_P (or F_{UHR}) and the Type 1 emission frequency. To answer these questions on the frequency selectivity of the Type 1 emissions, the following nonlinear wave-particle interaction has been considered to play an important role in the generation processes, that is expressed by,

$$\omega_{UHR} - \omega_1 - (k_{UHR} - k_1) \cdot V_b = n\Omega_e \qquad (n = 1, 2, ...) \qquad (2)$$

where Ω_e is the electron cyclotron angular frequency and the suffixes 'UHR' and '1' indicate the plasma wave in $F_P < F < F_{UHR}$ branch, and the Type 1 emission respectively. In the condition of the nonlinear wave-particle interaction given by eq. (2), the ESCH wave with the k-direction of 89° has been selected from the dispersion curves given in Fig. 10, to be excited at the frequency of about $3.4 F_H$ for the electron beam energy of 2 keV and the k-direction of 60° for the UHR waves. This frequency is lower than F_P by $0.6 F_H$. Though more quantitative calculations are required for the detailed investigation, it is quite probable that the nonlinear wave-particle interaction is concerned with the frequency selectivity of the Type 1 emissions. This nonlinear wave-particle interaction process has also been observed in the magnetosphere by EXOS-B (JIKIKEN) satellite and called the 'subsidiary emission'; the results will be published elsewhere in detail.

7.   ESLEC Mode Waves

The observation of the Type 2 emission by the S-310JA-6 rocket experiment has been made under the following conditions of the aurora and the particle precipitations.

1)   Type 2 emissions were observed both inside and outside of the auroral arcs.

2)   There was no clear correspondence between the Type 2 emissions and observed enhancements of the electron flux, and no remarkable relation to the energy spectrum. The trapped-type electrons, enhanced in the direction perpendicular to the magnetic field, were, however, predominant in the period of the ascent. These particles seem, therefore, to be correlated with these emissions.

3)   The auroral X-ray ($E > 20$ keV), measured simultaneously on the same rocket indicated a sudden enhancement by more than 2 factors in the period from 180 to 192 s (KODAMA, private communication). This enhancement of X-ray may have a relation to the burst-like intensification of the Type 2 emissions observed in the period from 167 to 198 s.

As has already been given in Section 4, the Type 2 emissions are identified to be the whistler mode waves or the ESLEC mode waves. The close correspondence between the Type 2 emissions and the electron beams in the aurora was not observed in the electron energy range of several keV (see Fig. 12 and also Fig. 13). We can con-
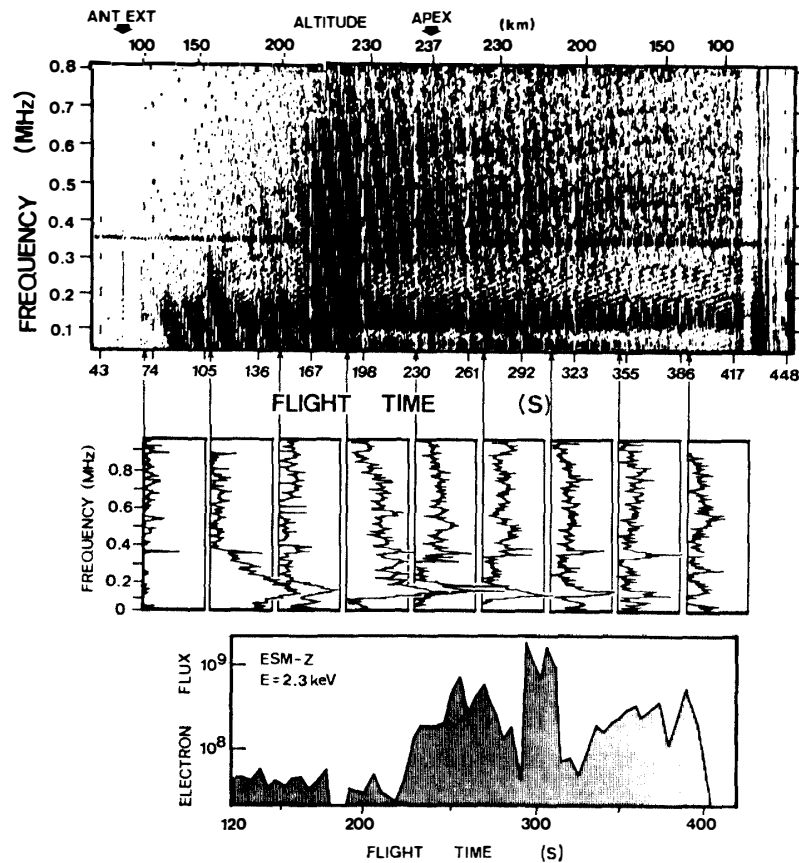
Fig. 13. Expanded dynamic spectrum of the emissions, in a frequency range below 0.8 MHz, with the ampligram of the emissions and the flux of the energetic electrons with the field-aligned pitch angle $(3.5° < \alpha < 17.5°)$ at the energy of 2.3 keV.

clude with a high possibility that the Type 2 emission is not caused by the beam type interaction, but is due to the plasma instability process associated with the opposite extreme case of the velocity distribution of electrons such as loss-cone type distribution. The generation of the electrostatic waves around $0.5 F_H$ has been historically suggested for the particle distributions enhanced in the direction perpendicular to the magnetic field (SHIMA and HALL, 1965; YOUNG, 1974; KARPMAN et al., 1975). Therefore, it is fairly possible that the generation mechanism of the Type 2 emission can be attributed to the loss-cone instability by the energetic electrons which have the pitch angle anisotropy enhanced in the direction perpendicular to the magnetic field. This conclusion also coincides with the previous result observed by S-210JA-21 (OYA et al., 1980). Since the k value of this plasma wave due to the loss-cone instability is large, we can conclude that the Type 2 emissions are the ESLEC mode waves rather than the whistler mode waves.

8. Ionospheric Continuum Emissions

The observation of the Type 3 emissions by the S-310JA-6 rocket has been made in the following situation relating to the aurora and the precipitating particles.

1) The Type 3 emissions were observed in a bright auroral arc.

2) The occurrence of the emissions coincides with the period of the maximum enhancement of the energetic electrons in all the energy channels.

3) The energy spectrum of the precipitating electrons during the period of this emission had a plateau in the spectrum ($\partial F(E)/\partial E \simeq 0$) in the energy range from 1 keV to 3 keV.

As has been described in Section 4 already, the emission has the broad-band characteristics that can be interpreted by the two possibilities; the first is the hypothesis of the continuum emission generated from the relatively wide range of the ionosphere in the topside, and the second is the possibility of the solar Type III radio burst.

At each corresponding level of the ionosphere, the upper hybrid mode waves ($F_P < F < F_{UHR}$, see Fig. 9) can be generated due to the high density beam of about $10^9/cm^2 \cdot s \cdot sr \cdot keV$ with the peak energy of approximately 2 keV. The generated UHR mode waves can be changed to the electromagnetic waves by the linear mode conversion process. The schematic interpretation of this mechanism is shown in Fig. 14. When these electrostatic waves propagate toward the higher density region of electrons, these waves can approach to the region where the wave frequency coincides with the local electron plasma frequency. In this region, a large part of the Poynting energy of the electrostatic waves can be converted to the L-O mode electromagnetic waves (Oya, 1974). As indicated in Fig. 14, when the linear conversion takes place effectively at the various altitudes in the topside ionosphere during the maximum enhancement of the electron precipitation, the electromagnetic waves with the wide frequency band, nearly from the local plasma frequency to the upper hybrid frequency at the ionospheric peak, should be observed at the position of the rocket in the topside ionosphere.

Recently, an observational evidence has been found, which clearly indicates the results of the linear mode conversion process in the lower ionosphere below the ionospheric peak. In this observation, wide-band radio waves emitted from the auroras were observed in the frequency range from 2.5 MHz to 6 MHz at the ground station (Kellogg and Monson, 1979). The critical frequency of the E-layer, measured by the bottomside sounding, was about 12 MHz. Therefore, these emissions are considered to be electromagnetic waves which have been excited by the auroral electrons as the electrostatic mode waves. The generated electrostatic waves were subjected to the linear mode conversion from the electrostatic to the electromagnetic mode at the lower ionosphere.
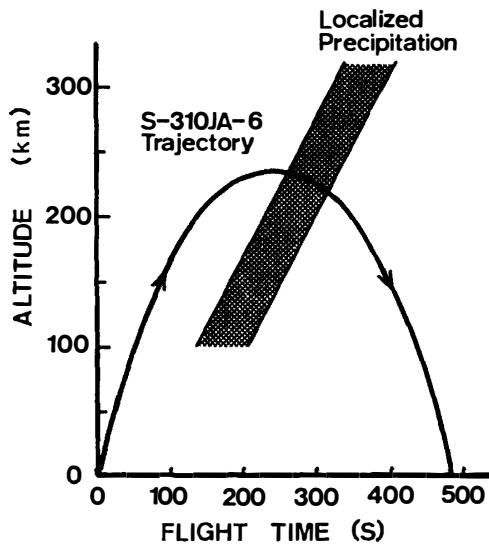
Fig. 14a. Geometrical relation of the localized precipitation region close to the period of the broad-band HF emission to the rocket trajectory in the S-310JA-6 experiment.
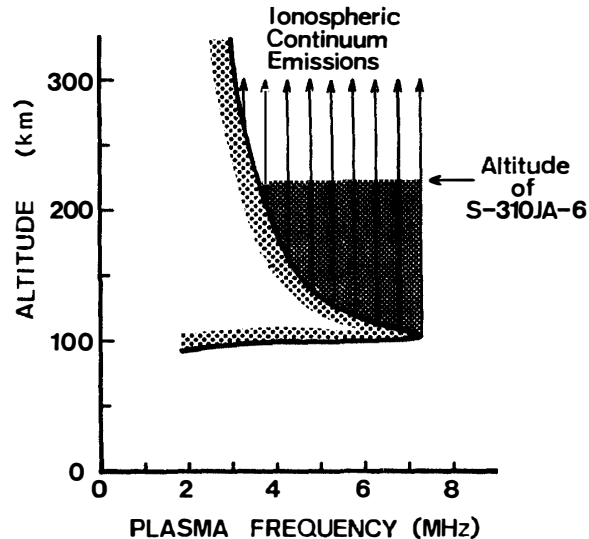
Fig. 14b. Schematic interpretation of the possible wide-band spectrum of the Type 3 emission. The emissions emanated from various altitudes of the ionosphere can be detected as the wide-band spectrum with the lower cutoff at the local plasma frequency.

One unsolved question to this continuum hypothesis is why the upper limit frequency of the continuum emission has been always constant and ended at the maximum limit of the PWH equipment, though the precipitating electrons that control the peak density of the ionosphere have varied so rapidly.

There still remains a possibility of the radio source from the outside of the earth as a case of solar Type III bursts. Though the rocket flight was made in the midnight, the long-distance propagating electron beam from the sun becomes possible to be seen from the nightside region of the earth. This is because the Type III burst is generated along the Archimedian spiral of the interplanetary magnetic field. No complete identification is possible because a wide variety of combinations, to provide the chance for the observation of the radio waves from the celestial bodies outside of the earth, can be considered. There is a limitation for identifying the radio wave from the celestial origin by a rocket experiment that is carried out merely for a limited short period.

9. Leaked AKR Emissions

In the two rocket experiments carried out by the S-310JA-4 and S-310JA-6

rockets, the emissions around 200 kHz have unique characteristics; *i.e.*, the emission is observed always after the rockets have penetrated through the ionospheric level where the local plasma frequency coincides with the emission frequency. The emissions have been terminated again when the rockets passed through the ionospheric level where the plasma frequency becomes approximately the same as the emission frequency.

In both the cases of S-310JA-4 and the Type 4 emissions in the S-310JA-6 experiment, no correlation between the *in situ* observations of the energetic particles and the emissions has been identified. The emissions are also observed without effects from the local breakup of the aurora. All these features lead us to a conclusion that the emission is not a local origin but the propagating whistler mode wave which came from the outside region of the ionosphere.

Recently, extensive studies on the radio waves outside the ionosphere have been achieved. Considering all these results of the existing emissions outside the ionosphere, the most possible source of this Type 4 emission observed by S-310JA-6 (we consider hereafter the emission observed by S-310JA-4 near at 200 kHz to be the same category of the phenomena) is the auroral kilometric radio wave that is generated at the altitude from 6000 km to 10000 km above the ionosphere along the magnetic field line in the auroral region. The basic feature of the auroral kilometric radio wave (ARK) in the calm period of the geomagnetic activity, consists of nearly constant dynamic spectrum at around 200 kHz to 300 kHz; *i.e.*, quite similar spectrum pattern to the Type 4 emission. The AKR emission indicates the intensification and the broadening of the bandwidth when the substorm starts.

The electron beams with an energy of several keV are expected to excite electromagnetic and electrostatic plasma waves in the two frequency bands; $F < \min(F_P, F_H)$ and $\max(F_P, F_H) < F < F_{UHR}$ as already shown in Fig. 10. In consequence, there are two candidates for the generation mechanism of the Type 4 emission, corresponding to these two frequency bands in which emissions can be excited originally.

The first is a case of the wave excitation in the frequency band $F < \min(F_P, F_H)$. Since the frequency of the emission is in a range from 100 kHz to 300 kHz, the region that satisfies this condition should be located in the plasmasphere where the plasma frequency is larger than 300 kHz. The excited waves in this frequency band can propagate and reach the low-altitude ionosphere directly as the whistler mode waves. This is equivalent to the generation mechanism of the auroral hiss emissions (MAGGS, 1976, 1978). In this mechanism, however, we cannot interpret the narrow band spectrum of the Type 4 emissions. According to the calculation of the power spectrum for the waves excited in this frequency range (MAGGS, 1978), the power flux is expected to have a sharp peak value at the frequency about $2F_{LHR}$, where F_{LHR} is the lower hybrid resonance frequency, and decreases monotonously with increasing frequency up to the frequency of $\min(F_P, F_H)$. F_{LHR} is lower than approximately 10 kHz in the region from the polar ionosphere to the magnetosphere.

We cannot, therefore, interpret the narrow-band characteristics of the Type 4 emission observed at the frequency about 100 kHz to 200 kHz.

There is also a clear reason why we could not observe the broad-band emission in this frequency range. That is, the possible source region for this category of the mechanism, is located inside the plasmasphere, where no significant injection of the beam electrons is feasible. When the source energy is related to the beam type electrons, the source region should be located in the trough region with $F_H \gg F_P$. The only candidate to give the frequency range from 100 kHz to 300 kHz is, then, the case of $F_H < F < F_{UHR}$.

The electrostatic plasma waves excited in the frequency range, $F_H < F < F_{UHR}$, are expected to be the effective source for the intense electromagnetic radiations through the linear mode conversion process, for example auroral kilometric radio waves (AKR), nonthermal continuum radiations, Jovian hectometric and decametric radio waves (OYA, 1974; BENSON, 1975; JONES, 1976, 1977).

In the present case of the Type 4 emission, the observations were made in the earth's ionosphere; the mode conversion into the whistler mode branch becomes important at the local plasma frequency. The generation and conversion mechanism of the Type 4 emission is shown schematically in Fig. 15. The original electrostatic plasma waves are considered to be excited in the frequency range of $F_H < F < F_{UHR}$ by the auroral electron beams which are accelerated in the V-shaped potential region above the polar ionosphere. While the AKR emissions (electromagnetic mode waves) are generated, having been converted from the electrostatic mode (UHR waves in Fig. 15) in the conversion region where the wave frequency coincides with the local electron plasma frequency, the Type 4 emissions are produced as a result of the mode conversion to the whistler mode waves that can propagate downward to the lower ionosphere. As a consequence, these down-going whistler mode emissions are considered to be the leaked component of AKR through the polar ionosphere. Here we call this Type 4 emissions leaked AKR emissions. The center frequency and the bandwidth of the leaked AKR emissions coincide, therefore, with the original AKR emissions.

A typical example of AKR power spectra observed by JIKIKEN (EXOS-B) satellite is shown in Fig. 16. In this figure, it is clear that AKR has a bandwidth approximately 100 kHz around the center frequency of about 200 kHz. This frequency structure is quite consistent with the observed spectrum of the Type 4 emissions.

It cannot be confirmed for this case whether AKR was active or not in the polar magnetosphere at the same time as the rocket experiments, because the *in situ* satellite observations could not be carried out. From many correlative studies between AKR and auroral activity, however, AKR has been considered to be always active when the discrete auroral arcs are present in the nightside polar ionosphere (GURNETT, 1974; MORIOKA and OYA, 1980). As summarized in Table 2, the two rocket experi-
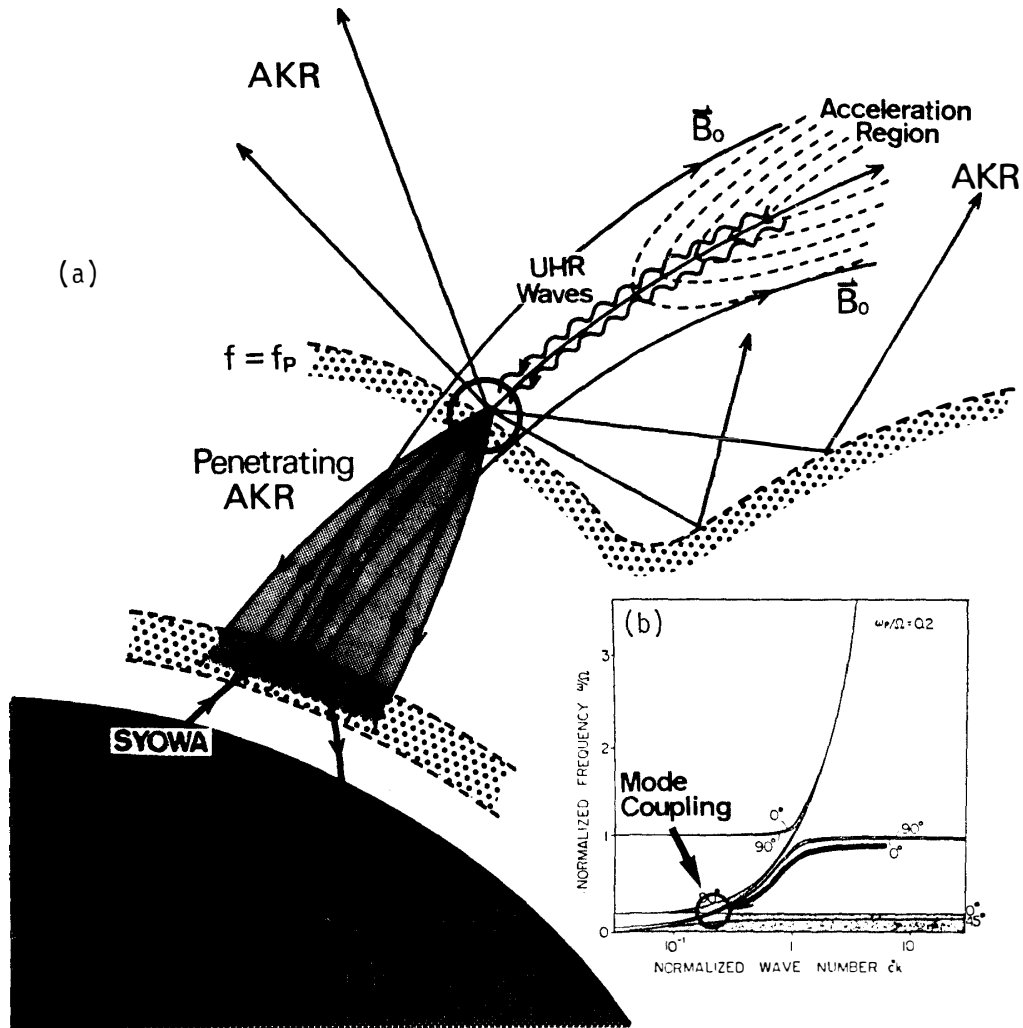
Fig. 15. (a) Schematic interpretation of the generation and propagation processes of the leaked AKR emission. In the region where the wave frequency coincides with the local plasma frequency, the mode conversion from the Z-mode waves to the whistler mode waves takes place, these converted waves can propagate down to the lower ionosphere in the form of the whistler mode waves.

(b) ω-k diagram of the plasma waves in the generation region of AKR. The mode conversion takes place when the wave frequency coincides with the local plasma frequency.

ments were carried out both in the period from the substorm onset to the expansion phase, and auroras were also observed in both cases. Consequently, it is quite probable that AKR was present in the polar magnetosphere at the same time as the rocket experiments.
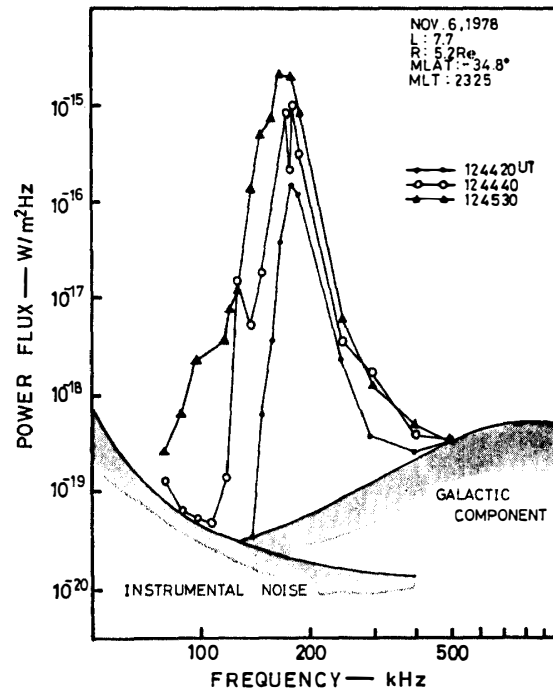
Fig. 16. *Power spectra of auroral kilometric radio waves (AKR) observed by JIKIKEN (EXOS-B) satellite in the magnetosphere. It is clear that AKR has a bandwidth about 100 kHz around a center frequency of nearly 200 kHz (after MORIOKA and OYA, 1980).*

10. Conclusion

The electric field component of the plasma waves and the electromagnetic waves has been successfully observed in the E and F_1 regions of the polar ionosphere using the S-310JA-4 and S-310JA-6 rockets launched at 0332 LT (45°E) on August 18, 1978 and at 0056 LT (45°E) on August 28, 1978, respectively from Syowa Station. The successful operation of the on-board PWH (plasma wave detector in HF range) equipments have provided four different types of the emissions.   Since the S-310JA-6 rocket was fired into the fairly active region of the aurora, we have obtained the dynamic spectra of all these four types of the emissions, while only one type of the emission from 200 kHz to 300 kHz was observed by the S-310JA-4 rocket that could not approach to the activity center of the auroral breakup.

The observed four types of the emissions are analyzed by investigating the condition of the wave-particle interactions that is effectively carried out using the data of the precipitating energetic electron energy spectra coupled with the plasma wave dispersion curves calculated on the basis of the measured plasma parameters, such as the electron density and the electron temperature.

The observed four types of emissions are identified about their modes and the possible generation mechanism as summarized in Table 3.   The Type 1 emission that is identified to be the subsidiary emission is essentially produced by the beam instability on the ESCH waves.   Due to the effective growth in a large k domain,

Table 3.   Summary of the emissions observed in the rocket experiments.

Emis-sion type	Observation		Frequency range	Correlation with energetic electrons	Wave mode (ES/EM)	Generation mechanism
	S-310					
	JA-4	JA-6				
Type 1	×	○	$F_P - F_H$ ($2F_H$) 2~5 MHz	Precipitating component ($\alpha \sim 0°$)	ESCH waves lower than F_P (Subsidiary emission)	Beam instability + Nonlinear wave-particle interaction
Type 2	×	○	$(0.2 \sim 0.6)F_H$ 200~700 kHz	Trapped component ($\alpha \sim 90°$)	ES waves lower than F_H (ESLEC mode waves)	Loss-cone instability
Type 3	×	○	$F \gtrsim F_P$ $F \gtrsim 3$ MHz	Maximum enhancement period	L-O mode EM waves (Ionospheric continuum emission)	Beam instability + Linear mode conversion ($\rightarrow$ EM waves)
Type 4	○	○	$(0.1 \sim 0.2)F_H$ 100~200 kHz	Weak correlation	Whistler mode waves (Leaked AKR)	Beam instability + Linear mode conversion ($\rightarrow$ Whistler mode waves)

the generation mechanism is put in the regime of the nonlinear wave-particle inter-actions.   The Type 2 emission is identified to be the ESLEC mode waves; we defined, in this paper, the electrostatic plasma waves in the frequency range lower than the electron cyclotron frequency as the ESLEC waves.   The ESLEC mode wave is generated by the loss-cone type particles and not necessarily related to the auroral breakup that causes the beam type electron precipitation.   The most possible mecha-nism of the Type 3 emission is the continuum emission emanating from the iono-spheric level lower than the rocket position.   The generated upper hybrid mode electrostatic waves may possibly be converted into the L-O mode electromagnetic waves.   There, however, remains a possibility of the HF radio waves from the celestial sources such as the solar Type III burst from the interplanetary space apart from the sun.   Details still remain for future studies.

The discovery of the leaked AKR emission is an important result of this paper. The Type 4 emission is identified as the whistler mode wave that is converted from the electrostatic plasma wave of the upper hybrid mode.   From the origin of AKR emissions, a part of the wave energy leaked downward to be converted into the whis-tler mode waves.

It is rather surprising that in a relatively narrow region of the lower part of the polar ionosphere, all types of the essential process of the plasma wave generation mechanisms are taking place in relation to the auroral activities.   Considering the

energy range of the interacting particles, the original modes of the plasma waves are electrostatic. The high energy density of these electrostatic mode waves is converted to the electromagnetic waves through the corresponding conversion mechanisms. Part of the emissions can be still observed in the form of the original electrostatic plasma waves.

Acknowledgments

References

BENSON, R. F. (1975): Source mechanism for terrestrial kilometric radiation. Geophys. Res. Lett., 2, 52–55.

GURNETT, D. A. (1974): The earth as a radio source: Terrestrial kilometric radiation. J. Geophys. Res., 79, 4227–4238.

HIRASAWA, T. and NAGATA, T. (1972): Constitution of polar substorm and associated phenomena in the southern polar region. JARE Sci. Rep., Ser. A (Aeronomy), 10, 76 p.

JONES, D. (1976): Source of terrestrial non-thermal radiation. Nature, 260, 686–689.

JONES, D. (1977): Mode-coupling of Z-mode waves as a source of terrestrial kilometric and Jovian decametric radiations. Astron. Astrophys., 55, 245–252.

KARPMAN, V. I., ALEKHIN, JU. K., BORISOV, N. D. and RJABOVA, N. A. (1975): Electrostatic electron-cyclotron waves in plasma with a loss-cone distribution. Plasma Phys., 17, 361–372.

KELLOGG, P. J. and MONSON, S. J. (1978): Rocket observation of high frequency waves over a strong aurora. Geophys. Res. Lett., 5, 47–50.

KELLOGG, P. J. and MONSON, S. J. (1979): Radio emissions from the aurora. Geophys. Res. Lett., 6, 297–300.

MAGGS, J. E. (1976): Coherent generation of VLF hiss. J. Geophys. Res., 81, 1707–1724.

MAGGS, J. E. (1978): Electrostatic noise generated by the auroral electron beam. J. Geophys. Res., 83, 3173–3188.

MORIOKA, A. and OYA, H. (1980): Auroral kilometric radiation and magnetospheric substorm—

Results from JIKIKEN observation. Uchû Kansoku Shinpojiumu, Showa-55-nendo. Tokyo, Tokyo Daigaku Uchû Kôkû Kenkyu-jô, 436–455.

OYA, H. (1971): Conversion of electrostatic plasma waves into electromagnetic waves: Numerical calculation of the dispersion relation for all wavelengths. Radio Sci., 6, 1131–1141.

OYA, H. (1974): Origin of Jovian decameter wave emissions—Conversion from the electron cyclotron plasma wave to the ordinary mode electromagnetic waves. Planet. Space Sci., 22, 687–708.

OYA, H., MIYAOKA, H. and MIYATAKE, S. (1979): Nankyoku roketto S-310JA-1, 2-gôki ni yoru kôshûhatai denpa hôsha no kansoku—PWH no kansoku kekka (Observation of HF plasma wave emissions at ionospheric level using sounding rockets S-310JA-1, 2 in Antarctica). Nankyoku Shiryô (Antarct. Rec.), 64, 30–41.

OYA, H., MIYAOKA, H. and MIYATAKE, S. (1980): Nankyoku roketto S-210JA-21-gôki ni yoru kôshûha purazuma hadô supekutoru no kansoku (Observation of HF plasma wave spectrum at ionospheric level using sounding rocket S-210JA-21 in Antarctica). Nankyoku Shiryô (Antarct. Rec.), 69, 37–51.

SHIMA, Y. and HALL, L. S. (1965): Electrostatic instabilities in a plasma with anisotropic velocity distribution. Phys. Rev., 139, A1115–A1116.

YOUNG, T. S. T. (1974): Electrostatic waves at half electron gyro-frequency. J. Geophys. Res., 79, 1985–1988.